Desalination and Water Treatment
www.deswater.com

doi: 10.5004/dwt.2017.20118

75 (2017) 1–9
May

CCD series no. 23: theoretical model performance of BWRO desalination with CCD and multi-stage PFD of identical four-element modules under the same conditions

Avi Efraty

Desalitech Ltd, P.O.Box 132, Har-Adar, 90836, Israel, email: avi@desalitech.com

Received 15 November 2015; Accepted 1 February 2017

ABSTRACT

The principal goals of the modern brackish water reverse osmosis (RO) desalination (BWRO) industry are aimed at high recovery, low-energy processes in order to save water and energy, and minimize handling needs of brine effluents, and the newly emerging closed circuit desalination (CCD) technology under fixed flow and variable pressure conditions meets this targets economically already today with lower propensity of fouling and scaling compared with conventional plug flow desalination (PFD) techniques. The present study applies a theoretical model simulation database to compare between the performance of CCD and multi-stage PFD processes in design configurations of identical modules under the same flux and flow rates conditions. Exemplified with 2,000 ppm NaCl feed and designs comprising four-element modules, the present study reveals that CCD proceeds with lower specific energy (SE) compared with a perfect multi-stage PFD process without energy recovery means, and that the SE gap between said processes declines meaningfully only beyond the 90% recovery level. The SE data of the compared processes is also manifested by their entropy efficiencies. The comparative study also reveals that the average total dissolved salt of permeates derived by CCD is invariably higher than that of the multi-stage PFD process, due to the sharp exponential rise of CCD cycles compared with PFD stages with recovery. Most currently practiced BWRO is based on a conventional two-stage PFD design for 75%–80% recovery with some energy saving by turbocharge means and for such common applications the adaptation of CCD will allow higher recovery with lower energy and less fouling.

Keywords: Brackish water RO desalination; Low-energy BWRO; High recovery BWRO; Multi-step plug flow BWRO desalination; Closed circuit BWRO desalination; Entropy efficiency of BWRO desalination

1. Introduction

Depletion/deterioration of freshwater (FW) surface/ground sources on earth due to increased demand/consumption by expanding global population and increased standard of living, adverse regional climate changes, and growing pollution have created increased reliance on reverse osmosis (RO) desalination of seawater (SWRO) and brackish water (BWRO) for the creation of FW supplements and for the treatment of water supplies for various application. RO is thermodynamically favoured [1] over alternative desalination techniques since requires much less energy and, therefore, preferred economically. Future goals of the desalination industry [2] are directed towards RO processes of higher recovery, lower energy, and reduced fouling in order to save water and energy, and minimize handling needs of brine effluents and reduce operational expenses. It is impossible to reach these goals with conventional plug flow desalination (PFD) techniques, which remained essentially unchanged since inception by Loeb and Sourirajan [3] and practiced today at near state-of-the-art level with advanced membranes and efficient pumps and energy recovery devices (ERD) with very little room left for further improvements. Most (>90%) RO desalination practiced today relates to low salinity water treatment processes and BWRO where high recovery with low energy is an important parameter; whereas, in case of high salinity SWRO processes [4] of 45%–50% recovery, the emphasis is on energy saving, which strongly influences the cost of permeates.

Meeting future goals of the desalination industry necessitates new RO techniques, and in this context noteworthy are the recently emerging closed circuit desalination (CCD) methods for seawater [5–15] and brackish water (BW) [16–25], which proceed on the basis of different operational principles than those of conventional PFD techniques [26]. CCD is a batch desalination process carried out under fixed-flow and variable pressure conditions with recycling of the entire concentrate and its dilution with fresh pressurized feed at module(s) inlet(s). CCD recovery depends on the extent of concentrate recycling irrespective of number of elements per module, and energy consumption proceeds progressively as function of batch recovery with near absolute energy conversion efficiency in the absence brine release and, therefore, without need for ERD. Commercial application of CCD was made possible by the development of consecutive sequential batch desalination techniques to allow the occasional replacement of brine by fresh feed such as by the engaged/disengaged of a side conduit, or by incorporating into CCD processes for BW desalination brief PFD steps for flush out of brine without stopping desalination.

Experimental performance data of CCD units most of which comprise four-element modules (ME4) revealed high recovery low-energy processes [5–25] of high consistency with theoretical model simulations, which meet already today most of the future goals of the desalination industry. A recent theoretical study by Lin and Elimelech [27] analyzes the minimum specific energy (SE) of desalination dependence on the number of stages of conventional multi-stage PFD and CCD processes in an attempt to elucidate the fundamental differences between them, and concluded "… that although it is theoretical impossible to reach the thermodynamic minimum energy of separation with closed-circuit RO, this configuration is robust and much more practical to implement than the multi-stage direct pass RO". Rigorous theoretical model simulations for seawater desalination with single-element modules (ME) by CCD and multi-stage PFD in the flux range (13.0–0.1 LMH) under the same flow conditions revealed [15] that the former behaves as a near perfect multi-stage PFD process and proceeds with near absolute energy conversion efficiency. This study also revealed the fundamental differences between CCD cycles and PFD stages and their effects on RO desalination.

The present theoretical model study evaluates the performance of CCD and multi-stage PFD systems with identical ME4 under the same flow conditions in an attempt to ascertain the principal fundamental differences between them. The selection of the ME4 in this study coincides with the fact that most of the reported [16–25] CCD systems for BW make use of such a module configuration of high production efficiency of its individual elements.

2. Model designs of multi-step PFD and CCD with ME4

The design in Fig. 1(A) for batch CCD of BW is of a single module apparatus with four elements for fixed-flow variable pressure operation with set-points of flux, cross flow, and batch recovery. Making to the batch CCD process in the apparatus in Fig. 1(A) into a continuous consecutive sequential process can be achieved by means of the design in Fig. 2 with a side conduit that can be engaged occasionally with the closed circuit for brine replacement by fresh feed with negligible losses of energy as already exemplified experimentally [5,6]. The performance of the batch (Fig. 1(A)) and the consecutive sequential batch (Fig. 2) apparatus is typical of a continuous flow-staged and pressure-boosted conventional multi-stage PFD configuration with ME4 of the type displayed in Fig. 1(B). The differences between the batch CCD (Fig. 1(A)) and multi-stage PFD (Fig. 1(B)) processes arise from the dilution effect associated only with cycles of the former; the near absolute energy conversion efficiency of the former in the absence of brine release and need for ERD; and the simple design of the former in contrast with the complexity of the latter with its many modules and inter-stage booster pumps. A conventional two-stage PFD process

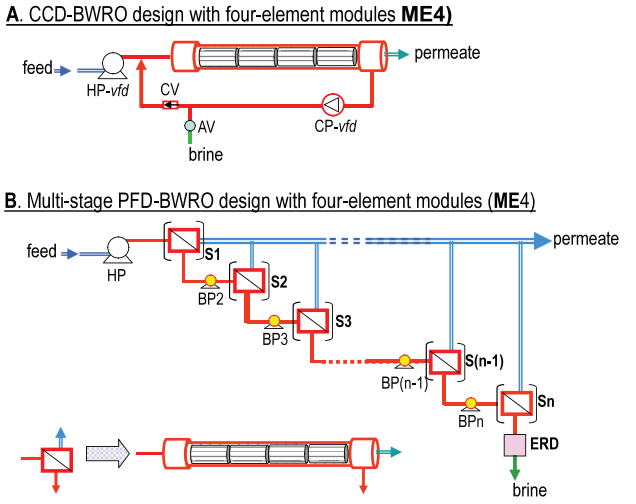

Fig. 1. Schematic illustration of a single-module BWRO-CCD batch apparatus (A) and a conventional multi-stage BWRO-PFD system both with four-element modules (ME4).
Note: HP – high pressure pump; CP – circulation pump; vfd – variable frequency derive; AV – actuated two-way valve means; CV – one-way check valve means; S – stage; BP – booster pump; and ERD – energy recovery means.

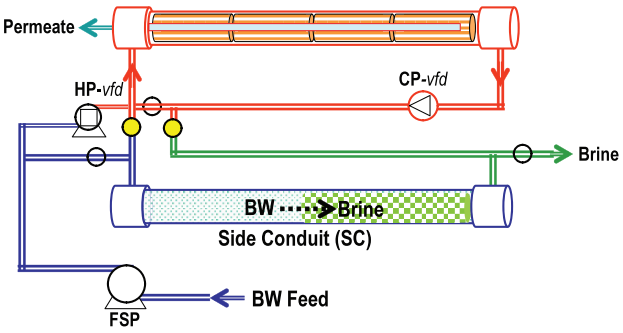

Fig. 2. Schematic illustration of a CCD apparatus with a single module of four elements and a side conduit (SC) showing a disengaged SC undergoing brine replacement by fresh feed supplied by the feed supply pump (FSP) at near atmospheric pressure, and thereafter, the SC is sealed, pressurized hydrostatically by the closed circuit pressure, and left on stand-by for the next engagement.

of 75%–80% recovery is normally carried out with a turbocharge between the stages that utilizes the disposed brine flow of the two stages; whereas, increased staging (>2) makes use of BP between stages for pressure adjustments without ERD. Accordingly, an effective comparison between a multi-cycle CCD and multi-stage (>2) PFD processes should take account of the average performance of the two configurations for high recovery (>90%) in the absence of ERD with identical modules operated with the same flow rates, and such simulations are presented next. In order to meet the aforementioned conditions, the multi-stage PFD configuration should comprise many modules of a declined number per stage; whereas, in case of CCD the same average performance is attained already the level of a single-module design.

3. Theoretical model simulations of CCD and multi-stage PFD with ME4

The theoretical model simulation database for CCD according to the Fig. 1(A) design is displayed in Table 1(A) with each column in the table labeled at bottom by a number. Selected data at the top of the table (yellow squares) outline the module configuration (four-element per module), membrane type (ESPA2-MAX) and its test conditions: feed source concentration (0.20 NaCl typical of BW sources in the electric conductivity (EC) range 3,000–3,800 μS/cm), 20 LMH flux, 45% module recovery (MR) of 13.9% average element recovery well within the recommended range by the selected element manufacturer, temperature (25°C), efficiency of pumps (75% for HP, BP and CP), and the van't Hoff constant for conversion of percent concentrations to osmotic pressures (8.00 bar/%). The selected operational parameters lead to the listed theoretically calculated terms of flow rates (Q), module pressure difference (Δp), average MR per element (av-MR/element), average concentration polarization factor (av-*pf*), cycle time duration (min/cycle), and average permeate production per cycle (m^3/cycle). CCD module inlet concentrations per cycle (3A) are derived from the module outlet concentrations (4A) by means of mass balance, which takes into account of the dilution effect at module inlet. The applied pressure (p_a) per cycle (6A) is derived by Eq. (1); where, μ stands of flux, A for the permeability coefficient of the membrane, T_{CF} for temperature correction factor, $\Delta\pi_{av}$ for average osmotic pressure of concentrate, Δp for module pressure difference, p_p for permeate pressure release, and π_p for average osmotic pressure of permeates – the small terms p_p and π_p were ignored during the calculation. The average applied pressure (7A) is derived from the applied pressure per cycle (6A). The power expressions of pumps (8A–10A) are the products of pressure and flow, and the average power contribution in 11A is derived from the power of individual cycles in 10A. The average SE (ΣkWh/m^3) terms (13A) are derived from the flow rates of permeates (12A) and the average cumulative power (11A). The CCD batch recovery (R_{BR}) terms in the table (14A) are derived in accordance with Eq. (2) from the ΣV_p (batch sequence cumulative volume (Σm^3) of permeates and the cited intrinsic volume of the closed circuit (V_i = 78.8 L) at the top of the table). The permeate total dissolved salt (TDS) terms per cycle (15A) and average (16A) in the table are derived by Eq. (3), where C_p stands for permeate concentration, B for salt diffusion coefficient, and C_f for module feed concentration. The entropy efficiency (EE) terms (18A) are derived by Eq. (4), where $W_{least\text{-}min}$ stands for the least-minimum SE of separation under reversible infinitesimal flux conditions and W_{sep} for the actual SE of separation. The least-minimum SE is the minimum energy required to overcome the osmotic pressure of the source under reversible infinitesimal flux conditions, or 1.6 bar m^3 (0.044 kWh/m^3) for 0.2% NaCl of π_f = 1.6 bar.

$$p_a = \mu/A/T_{CF} + \Delta\pi_{av} + \Delta p/2 + p_p - \pi_p \quad (1)$$

$$R_{BR} = 100 \times \Sigma V_p / \left(\Sigma V_p + V_i\right) \quad (2)$$

$$C_p = B \times C_f \times pf \times T_{CF}/\mu \quad (3)$$

$$EE = 100 \times \left[W_{least\text{-}min}/W_{sep}\right] \quad (4)$$

The data presented in Table 1(B) pertains to a perfect multi-stage PFD process of identical ME4 (E = ESPA2-MAX) modules design (Fig. 1(B)) with flow rates per module (3B–5B) the same as for the CCD process. Module inlet (6B) and outlet (7B) concentrations per stage are defined by MR = 45%, the same as for CCD. The applied pressure (p_a) per stage in Table 1(B) (8B) is derived by Eq. (1) with the same selected flux (20 LMH) as for the CCD process, and the boosted pressure per stage (9B) is the applied pressure difference (Δp_{BP}) of successive stages. All the modules of the staged PFD design operate with identical flow rates, irrespective of stage-number, and the SE per stage is derived from the product of feed flow at module inlet and applied pressure divided by the permeate flow and expressed in the table (10B) in kWh/m^3 units. The average SE terms (11B) are derived from the SE per stage (10B) by accounting for the declined rate of permeates' production in subsequent stages. The percent EE terms of the staged process (12B) are derived by Eq. (4) as already explained for CCD. The SE of separation per stage (13B) and average (14B) are derived from the respective applied pressure terms (8B) and their average. The TDS per stage of permeates (15B) is derived by Eq. (3), and the TDS average (16B) takes into account of the declined flow rate of permeates' production of subsequent stages in the process. Recovery (17B) is derived from the appropriate module's concentration terms. The multi-stage process under review proceeds along the line of staged ME4 of same MR and the SE of the entire process manifests an average of all stages.

The simulated database in Table 1(A) for CCD and in Table 1(B) for the multi-stage PFD processes relate to the identical ME4 under the same operational conditions of flow, flux, MR and temperature and, therefore, allow the obtainment of reliable comparative data of fundamental significance. Incidentally, the same simulation database may also apply to compare related systems of different module configurations and flux conditions by adjusting the parameters at the stop of Table 1(A) database.

Table 1
Theoretical model simulation data for ME4 (E = ESPA2-MAX) in CCD (A) and multi-stage PFD (B) related to 2,000 ppm NaCl (1.6 bar π) desalination with MR = 45% and 20 LMH flux at cited temperature and efficiency of pumps

Test – ESPA2-MAX		Unit design		CCD parameters		Temperature		
40.8	m^2/element	1	Modules	0.200	% NaCl feed	Temperature	25°C	
45.4	m^3/d	4	Elements/module	20.0	LMH flux	TCF	1.000 factor	
1,500	ppm NaCl	430	cm long PV	3.26	m^3/h permeate (Q_{HP})			
10.5	bar applied pressure	20	cm diameter PV	45.0	% module recovery			
15	% recovery	15	litre element volume	3.99	m^3/h Q_{CP}			
25	Centigrade	5	% lines volume	7.25	m^3/h module inlet flow			
99.60	% salt rejection	78.8	litre per module	0.538	bar Δp			
9.3	bar NDP			1.18	min/cycle			
46.364	LMH flux	π (bar)-C(%)		0.0644	m^3/cycle of permeate		Pumps	
4.9854	LMH/bar – A	2,000	ppm NaCl, 0.20 %	0.139	av-MR/element		0.75	HP *eff.*
0.1456	LMH – B	1.60	bar osmotic pressure	1.049	*av-pf*		0.75	CP *eff.*
		8.00	π (bar)/C(%) - van't Hoff factor	2.22	Flow ratio(concentrate/permeate)		0.75	BP *eff.*

A: CCD simulation results

Steps and concentrations				CCD sequence cycles						CCD sequence combined				Permeate		EE, %
Mode	Cycle	Inlet, %	Outlet, %	Time, min	p_a applied bar	p_a applied av-bar	Power (kW) per cycle HP	CP	HP + CP	av, kW	Perm., m^3/h	av-SE, kWh/m^3	REC, %	Cycle, ppm	av, ppm	
CCD	0	0.20	0.20	0.0	6.0	6.0	0.720	0.079	0.800	0.883	3.26	0.270	0	22	22	16.43
CCD	1	0.20	0.36	1.2	6.6	6.6	0.803	0.079	0.883	0.883	3.26	0.270	45.0	22	22	16.43
CCD	2	0.29	0.53	2.4	7.7	7.2	0.932	0.079	1.012	0.947	3.26	0.290	62.1	31	26	15.32
CCD	3	0.38	0.69	3.6	8.8	7.7	1.061	0.079	1.140	1.012	3.26	0.310	71.1	41	31	14.34
CCD	4	0.47	0.85	4.7	9.8	8.2	1.189	0.079	1.269	1.076	3.26	0.330	76.6	51	36	13.48
CCD	5	0.56	1.02	5.9	10.9	8.8	1.318	0.079	1.398	1.140	3.26	0.349	80.4	60	41	12.72
CCD	6	0.65	1.18	7.1	12.0	9.3	1.447	0.079	1.526	1.205	3.26	0.369	83.1	70	46	12.04
CCD	7	0.74	1.35	8.3	13.0	9.8	1.575	0.079	1.655	1.269	3.26	0.389	85.1	80	51	11.43
CCD	8	0.83	1.51	9.5	14.1	10.4	1.704	0.079	1.784	1.333	3.26	0.408	86.7	89	55	10.88
CCD	9	0.92	1.67	10.7	15.2	10.9	1.833	0.079	1.912	1.398	3.26	0.428	88.0	99	60	10.38
CCD	10	1.01	1.84	11.8	16.2	11.4	1.961	0.079	2.041	1.462	3.26	0.448	89.1	109	65	9.92
CCD	11	1.10	2.00	13.0	17.3	12.0	2.090	0.079	2.170	1.526	3.26	0.468	90.0	118	70	9.50
CCD	12	1.19	2.16	14.2	18.4	12.5	2.219	0.079	2.298	1.591	3.26	0.487	90.8	128	75	9.12
CCD	13	1.28	2.33	15.4	19.4	13.0	2.347	0.079	2.427	1.655	3.26	0.507	91.4	138	80	8.77
CCD	14	1.37	2.49	16.6	20.5	13.6	2.476	0.079	2.556	1.719	3.26	0.527	92.0	147	84	8.44
CCD	15	1.46	2.65	17.8	21.5	14.1	2.605	0.079	2.684	1.784	3.26	0.546	92.5	157	89	8.13
CCD	16	1.55	2.82	19.0	22.6	14.6	2.733	0.079	2.813	1.848	3.26	0.566	92.9	167	94	7.85
CCD	17	1.64	2.98	20.1	23.7	15.2	2.862	0.079	2.942	1.912	3.26	0.586	93.3	177	99	7.59
CCD	18	1.73	3.15	21.3	24.7	15.7	2.991	0.079	3.070	1.977	3.26	0.606	93.6	186	104	7.34
CCD	19	1.82	3.31	22.5	25.8	16.2	3.119	0.079	3.199	2.041	3.26	0.625	94.0	196	109	7.11
CCD	20	1.91	3.47	23.7	26.9	16.8	3.248	0.079	3.328	2.105	3.26	0.645	94.2	206	114	6.89
CCD	21	2.00	3.64	24.9	27.9	17.3	3.377	0.079	3.456	2.170	3.26	0.665	94.5	215	118	6.69
CCD	22	2.09	3.80	26.1	29.0	17.8	3.506	0.079	3.585	2.234	3.26	0.684	94.7	225	123	6.49
CCD	23	2.18	3.96	27.2	30.1	18.4	3.634	0.079	3.714	2.298	3.26	0.704	95.0	235	128	6.31
1A	2A	3A	4A	5A	6A	7A	8A	9A	10A	11A	12A	13A	14A	15A	16A	17A

(*Continued*)

Table 1 (*Continued*)

B: Multi-stage PFD simulation results

Step		Module flow rates			Concentrations		Pressure		SE total with brine			SE separation		Permeate TDS		RO REC, %
Mode	Stage	Inlet, m^3/h	Perm., m^3/h	Outlet, m^3/h	Inlet, %	Outlet, %	p_a, bar	Δp_{BP}, bar	SE-stage, kWh/m^3	av-SE[a], kWh/m^3	EE, %	SE-stage, kWh/m^3	av-SE, kWh/m^3	Stage, ppm	av[a], ppm	
PFD	0	7.25			0.20	0.20	6.0		0.547	0.547	8.34	0.246	0.2461	22	22	0.00
PFD	1	7.25	3.26	3.99	0.20	0.36	6.6		0.547	0.547	8.34	0.246	0.2461	22	22	45.00
PFD	2	7.25	3.26	3.99	0.36	0.66	8.6	1.9	0.706	0.604	7.56	0.318	0.282	33	26	69.75
PFD	3	7.25	3.26	3.99	0.66	1.20	12.1	3.5	0.996	0.668	6.83	0.448	0.3374	54	30	83.36
PFD	4	7.25	3.26	3.99	1.20	2.19	18.5	6.4	1.522	0.738	6.18	0.685	0.4243	91	35	90.85
PFD	5	7.25	3.26	3.99	2.19	3.97	30.1	11.6	2.480	0.814	5.61	1.116	0.5626	159	41	94.97
1B	2B	3B	4B	5B	6B	7B	8B	9B	10B	11B	12B	13B	14B	15B	16B	17B

[a]Accounting for declined rate of permeate production of subsequent stages.

4. Results of the comparative theoretical model simulations of CCD and multi-stage PFD with identical ME4 under the same conditions

The comparative results of the CCD and multi-stage PFD desalination systems with identical ME4 (EESPA2-MAXC) for 0.2% NaCl (1.6 bar π) under the same operational flow conditions per module of 45% MR and 20 LMH flux with assumed 75% efficiency of pumps (HP, CP, and BP) according to the data in Tables 1(A) and (B) are displayed on the recovery scale in Figs. 3(A) and (B) for modules concentrations (A) and pressures (B); in Figs. 4(A) and (B) for SE (A) and EE (B); in Figs. 5(A) and (B) for TDS of permeates per step (A) and average (B); and in Figs. 6(A) and (B) as function of step-number (A) and residence time (B). The comparative performance of the analyzed systems under infinitesimal flux conditions (0.1 LMH) with assumed absolute efficiency of pumps (100%) is displayed in Figs. 7(A)–(C) in reference to pressures (A), SE (B), and EE (C). The results' differences take account of the dilution effect experienced only in CCD, the absence of ERD means for PFD, and the decrease permeate flow rate per stage in PFD in contrast with the constant permeation flow rate per cycle in CCD. The aforementioned implies that the cumulative permeate flow rate in the multi-stage PFD process is not a linear function of the stage-number but an exponential function, which takes into account the declined number of modules per stage, while the flow rates per module remain unchanged irrespective of the stage-number. In contrast to the multi-stage PFD process, the permeate flow rate in CCD remains constant irrespective of the cycle-number, and the cumulative permeate volume during this process is a linear function of the cycle-number.

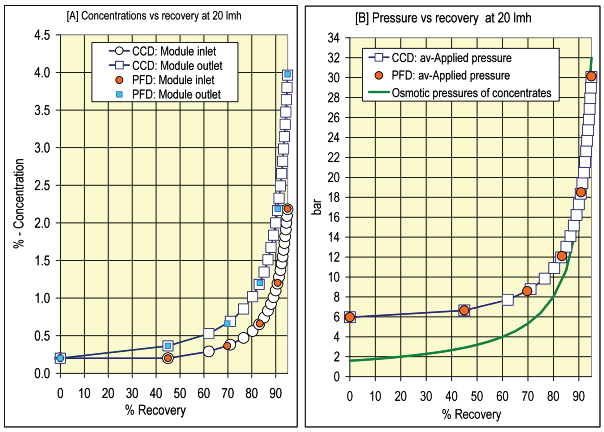

Fig. 3. Concentrations (A) and pressures (B) dependence on recovery for 95% desalination of 2,000 ppm NaCl with 45% MR and 20 LMH flux in the CCD (Fig. 1(A)) and multi-stage PFD (Fig. 1(B)) systems with identical ME4 according to the simulation database in Tables 1(A) and (B).

5. Discussion

The results of 95% desalination of 2,000 ppm NaCl by the compared CCD and multi-stage PFD systems designs (Figs. 1(A) and (B)) with identical ME4 under the same flow and flux conditions manifest the fundamental differences of their operational principles. In contrast to multi-stage PFD where fixed flow at module inlets is achieved by a declined number of modules per stage and fixed flux operation by an inter-stage BP with system recovery depending on the number of stages and the line of elements from start to end; CCD is a variable pressure batch process of fixed flow rates (HP and CP) controlled by set-points with full recycling of concentrates and recovery determined only by the number of closed circuit cycles irrespective of the number of elements per modules. The fundamental differences between the methods dictate their design features and performance characteristics, which are compared by the present model study with ME4 of identical flow rates and flux irrespective of method.

The incorporation of ME4 in the CCD and multi-stage PFD designs (Figs. 1(A) and (B)) for high desalination recovery implies the minimum need of just one module in the former in contrast to the requirement for many such modules in the later. The relative module-number per stage in the PFD design (Fig. 1(B)) under review can be derived from the expression $(1 - MR/100)^{n-1}$ where n stands for the stage-number and MR for module recovery, and for MR = 45% the relative numbers per stage (bold in parentheses) are as follows: 1.000 (**1**); 0.550 (**2**); 0.302 (**3**); 0.166 (**4**); and 0.0915 (**5**). Accordingly, a near perfect flow staged design

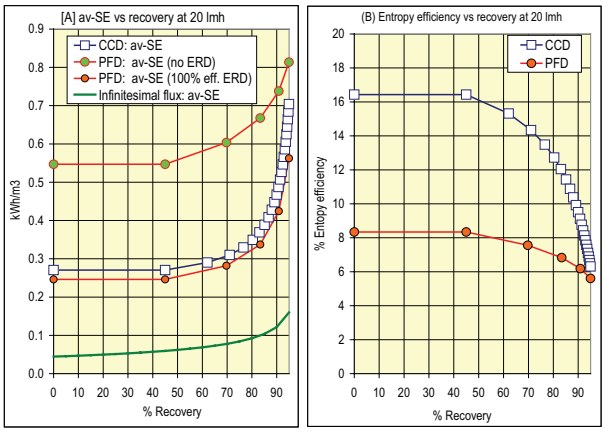

Fig. 4. Average SE (A) and EE (B) dependence on recovery for 95% desalination of 2,000 ppm NaCl with 45% MR and 20 LMH flux in the CCD (Fig. 1(A)) and multi-stage PFD (Fig. 1(B)) systems with identical ME4 according to the simulation database in Tables 1(A) and (B).

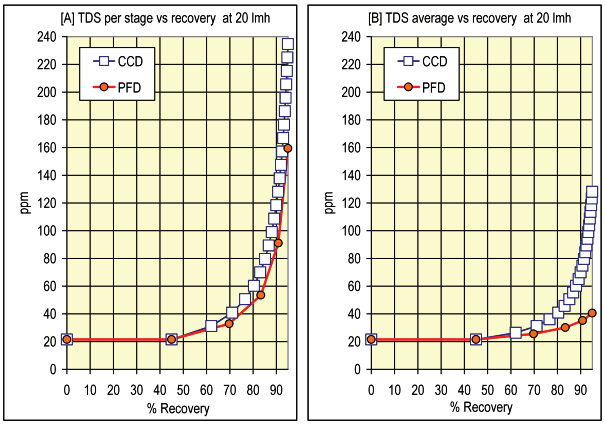

Fig. 5. Permeates' TDS per step (A) and average (B) dependence on recovery for 95% desalination of 2,000 ppm NaCl with 45% MR and 20 LMH flux in the CCD (Fig. 1(A)) and multi-stage PFD (Fig. 1(B)) systems with identical ME4 according to the simulation database in Tables 1(A) and (B).

in the context of the 5-stage PFD system under review in Table 1(B) would require 120 (**1**), 66 (**2**); 36 (**3**); 20 (**4**); and 11 (**5**) modules per stage with a total of 253 modules for the entire system. In simple terms, the multi-stage system comprises a complex design of many modules, and 4 BP would be required for a 5-stage design of 95% recovery in compliance with the performance data in Table 1(B), which makes this approach economically prohibited. Such 5-stage systems will remain complex and expensive even if the near perfect flow distribution is not attained, making this multi-stage approach of declined economic feasibility with increased stage-number. The aforementioned explains why most of the commonly used conventional BWRO systems are of a 2-stage design type, make use of six-element modules (ME6) of ~50% MR, and enable up to ~80% recovery without exceeding the stated specifications of membranes by their producers. Conventional 3-stage designs allow up to ~90% recovery and operate with 2 BP and without ERD.

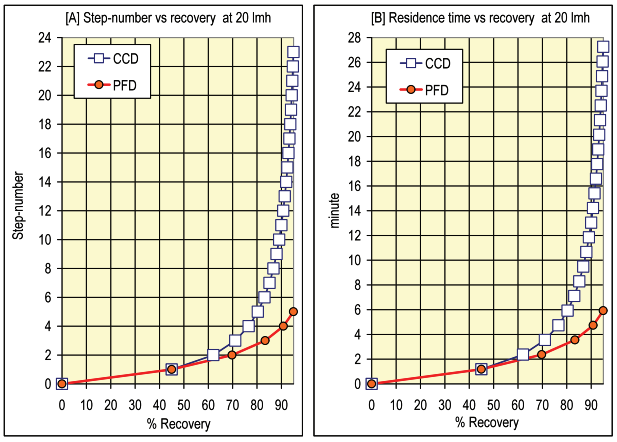

Fig. 6. Step-number (A) and residence time (B) dependence on recovery for 95% desalination of 2,000 ppm NaCl with 45% MR and 20 LMH flux in the CCD (Fig. 1(A)) and multi-stage PFD (Fig. 1(B)) systems with identical ME4 according to the simulation database in Tables 1(A) and (B).

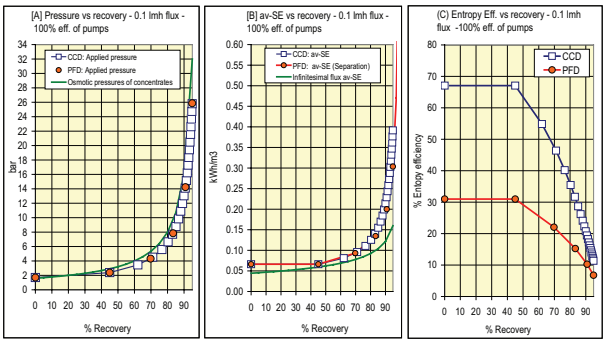

Fig. 7. Pressures (A), av-SE (B), and EE (C) dependence on recovery for 95% desalination of 2,000 ppm NaCl with 45% MR under near infinitesimal flux (0.1 LMH) conditions with absolute efficiency of pumps in the CCD (Fig. 1(A)) and multi-stage PFD (Fig. 1(B)) systems with identical ME4 according to the adjusted simulation database in Tables 1(A) and (B).

In sharp contrast with the multi-stage PFD designs, the simple CCD designs allow reaching the highest recovery per defined source under controlled flux and cross flow conditions already at the level of a single module, irrespective of its element-number. CCD production of permeates depends on the number of modules in the design with their inlets and outlets connected in parallel to the closed circuit.

The recovery depended performance of CCD and multi-stage PFD manifests the fundamental differences between closed circuit batch and continuous PFD and the nature of steps by which such processes proceed. In the absence of pressurized brine released during batch or continuous sequential batch CCD under fixed flow and variable pressure conditions, such processes proceed with near absolute energy conversion efficiency without need for ERD, and this in contrast to conventional PFD processes, including multi-stage, where part of the accumulated power in the system (HP and BP) is retained in the pressurized flow of the brine effluent and should be recovered in order to achieve high

energy efficiency. Noteworthy in particular are the different steps encountered in the compared processes with CCD cycles proceed with a concentrate dilution effect at module inlet with undistinguished flow rates between cycles; whereas, the multi-stage PFD process proceeds without a dilution effect but with declined flow rates per subsequent stage of declined weight on the average SE and the average TDS of permeates. The aforementioned in the context of the comparative theoretical model simulated data in Tables 1(A) and (B) and Figs. 3–6 is exemplified next.

The inlet and outlet concentrations dependence on recovery of the identical ME4 in the compared systems are the same (Fig. 3(A)) but proceed with a different step-number exemplified with a 5-stage PFD compared with a 23-cycle CCD requirements (Fig. 6(A)) to reach 95% recovery. The increased number of CCD cycles compared with PFD stages along the exponential concentration curves in Fig. 3(A) manifests a strong dilution effect in the ME4 at 45% MR only during the former process. Module concentrations define osmotic pressures and the required applied pressures (1) to sustain RO desalination at a desired flux, and this aspect is exemplified for 20 LMH in Fig. 3(B) by the same exponential applied pressure curves of increased frequency of CCD cycles compared with PFD stages. The exponential curve in Fig. 3(B) represents an average per step whereas under real conditions each individual pressure boost represents a step of unchanged pressure with more such steps required to reach a defined recovery by CCD cycles than by PFD stages. The reference curve in Fig. 3(B) of osmotic pressures of concentrates represents the applied pressure requirements under infinitesimal flux conditions with higher operational flux creating a larger pressure gap with the reference curve.

Power demand in RO depends on flow and pressure as well as on the efficiency of pumps, and the specific energies in the model systems (Fig. 4(A)) relate to av-SE CCD; av-SE PFD(no ERD); av-SE PFD(100% eff. ERD); and av-SE under infinitesimal flux as a minimum energy reference. The av-SE CCD curve in Fig. 4(A) is found slightly above that of the PFD multi-stage for water separation with absolute brine energy recycling (av-SE [100% eff. ERD]), and the small difference arises primarily from the small energy demand of the CP pump in CCD. Accordingly, CCD proceeds with near absolute energy conversion efficiency and energy demand typical of the water separation step in RO. Compared with the CCD, the actual av-SE of the multi-stage PFD process without ERD is much higher, and the gap between the methods declines with increased recovery (Fig. 4(A)) with minimum found at the 95% recovery level where brine energy losses in the system become lowest. The energy consumption trends in Fig. 4(A) of CCD < PFD with a declined gap with recovery are also manifested their EE curves (Fig. 4(B)), which take account of energy losses to the environment (e.g., brine energy) and/or due to increased irreversibility and/or due to declined efficiency of components. Since the data for the compared processes in Tables 1(A) and (B) pertains to modules of the same design, flow rates, and efficiency of pumps, the EE curves (Fig. 4(B)) show that CCD compared with the multi-stage PFD proceeds with a much higher EE in the beginning and a progressively declined gap with recovery and an ultimate merger at 100% recovery. The fast declined of EE in CCD with increased number of cycles implies increased entropy losses with recovery due to increased irreversibility arising from the dilution effect; however, EE of CCD remains higher than that of PFD irrespective of the magnitude the gap, and both become equal only at 100% recover.

Summary of the energy saving effect of CCD compared with that of the multi-step PFD configuration (Figs. 1(A) and (B)) under identical flux and flow rates conditions with identical ME4 according to the data in Tables 1(A) and (B) is exemplified in Fig. 8 with emphasis of PFD stages and CCD cycles. The first CCD cycle and PFD stage correspond to the same recovery (45%) since the dilution effect in the former starts only after the first cycle, and thereafter, more cycles than stages are required to reach a desired recovery as results of the dilution effect in the former process. The step fine-structure of cycles and stage and their relationship on the recovery scale are made clear in Fig. 8 and show the major energy saving benefits of CCD over multi-stage PFD up to 90% recovery, and thereafter, the energy saving benefit declines sharply due to the exponential rise in the number of the CCD cycles required to reach 95% recovery and the irreversibly entropy losses, which they create. Energy savings in favour of CCD as function of recovery in Fig. 8 are as follows: 0.28 vs. 0.55 (Δ = 0.27) kWh/m^3 for 0%–45%; 0.29 vs. 0.61 (Δ = 0.32) kWh/m^3 for 46%–61%; 0.31 vs. 0.67 (Δ = 0.36) kWh/m^3 for 70%; 0.35 vs. 0.67 (Δ = 0.32) kWh/m^3 for 80%; 0.48 vs. 0.75 (Δ = 0.27) kWh/m^3 for 90%; and 0.70 vs. 0.81 (Δ = 0.11) kWh/m^3 for 95%. The aforementioned figures translate to percent energy savings by CCD as function of recovery (bold in parenthesis) of 49% (**40%**); 52% (**50%–60%**); 54% (**70%**); 48% (**80%**); 36% (**90%**); and 14% (**95%**).

Permeates TDS of the compared CCD and multi-stage PFD simulated processes in Tables 1(A) and (B) are displayed in Figs. 5(A) and (B) as function of recovery and steps, and reveal a strong link with the number of steps required to reach a desired recovery above 45% recovery. Despite the moderate TDS rise per subsequent cycle due to the dilution effect in CCD, the exponentially increased number of

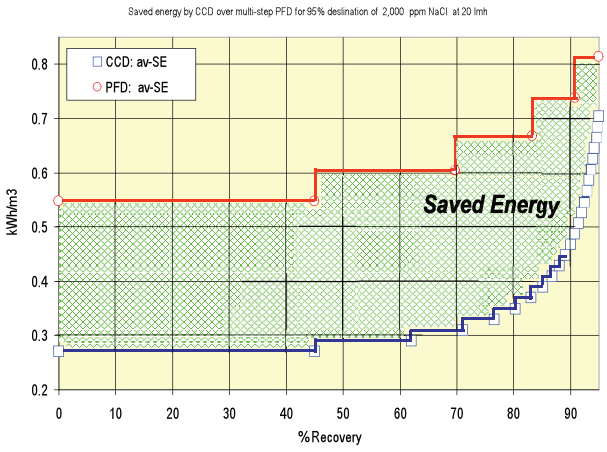

Fig. 8. The energy saving effect dependence on recovery for 95% desalination of 2,000 ppm NaCl with 45% MR and 20 LMH flux in the CCD (Fig. 1(A)) and multi-stage PFD (Fig. 1(B)) systems with identical ME4 according to the simulation database in Tables 1(A) and (B).

cycles required to reach a defined recovery with unchanged flow rates creates inferior permeates compared with the multi-stage PFD process where the stage-number is much smaller and the flow rates per stage decline rapidly with a decreased weight of produced permeates on the overall TDS. The declined permeate flow rate per stage in PFD implies the percentage contribution per stage (bold in parenthesis) to the total av-TDS of 53.9% (**1**); 9.6% (**2**); 11.2% (**3**); 12.2% (**4**); and 13.1% (**5**). In contrast to the multi-stage PFD process, in the fixed-flow CCD process the first cycle contributes 16.8% of the total av-TDS in the absence of a dilution effect, and thereafter, a fixed addition of 3.78% per cycle in the presence of a dilutions effect. Accordingly, the inferior permeates quality of relatively high av-TDS with increased recovery observed for CCD compared with the multi-stage process arise from the fundamental difference between the methods, which are manifested, amongst others, by the higher step-number (Fig. 6(A)) and grater residence time (Fig. 6(B)) in the CCD method.

The simulation database of the compared systems under consideration hereinabove was tested with flux of 0.1 LMH and absolute efficiency (100%) of pumps and ERD under which conditions the applied pressure curve should essentially merge with that of osmotic pressures of concentrates, and the same trend is also expected for the av-SE curves of CCD and the multi-step PFD processes. Moreover, under the assumed conditions the EE of each of the compared processes should reach its highest possible level. The comparative data furnished in Figs. 7(A)–(C) in reference to applied pressure (A), av-SE (B), and EE (C) is consistent and with the aforementioned expectations and, thereby, provides confirmation to the validity of the simulation database over a wide flux range and the trustworthiness of its projections.

The recent study by Lin and Elimelech [27] addresses the minimum desalination energy of CCD and multi-stage PFD for BW (5,000 ppm NaCl) desalination of 90% recovery and compares stage-number (n) effect on minimum-SE for n = 1, 2, 4, 8, and ∞. The present study shows that the multi-stage PFD process is fundamentally different from CCD; stage-number in the former and cycle-number in the latter have different physical meanings; and that comparison between such systems at the same stage-number and cycle-number could be misleading. Energy consumption (av-SE) by CCD under fixed-flow and variable pressure consecutive sequential batch conditions proceeds with identical flow rates of pressurized feed (HP) and permeate in the absence of any brine release and, therefore, could be estimated from the average applied pressure (av-p_a) by av-SE (kWh/m^3) ≈ (av-p_a)/36/eff_{HP} if the relatively small power consumption of CP is ignored. A previous study addressing the SWRO energy consumption of CCD compared with that of a multi-stage PFD design with identical ME revealed [15] that the former behaves as a near perfect 8-stage PFD system of similar energy consumption for 50% recovery at 13 LMH. The same study [15] also showed very similar specific energies for CCD units with ME and ME4 at 13 LMH and 50% recovery. The aforementioned implies that the low energy consumption in CCD is irrespective of number of elements per module and will proceed parallel to that of a perfect multi-stage PFD system of infinite stages (∞-stage).

6. Concluding remarks

The present study explores as an example the performance of the CCD and multi-stage PFD systems with identical ME4 under the same flow and flux conditions (20 LMH, 13.9% av-element recovery, 1.049 av-*pf*) up to 95% for feed of 2,000 ppm NaCl typical of common BW sources in the electric conductivity range of 3,000–4,000 μS/cm. Short ME4 allow high flux permeates' productivity characteristic of the four front elements in conventional ME6, and for this reason most of the reported CCD units for seawater [5–15] and BW [16–25] desalination comprise *n*ME4 designs where the respective inlets and outlets of n modules are connected in parallel to the closed circuit. The present study reveals a clear energy saving preference of CCD over multi-stage PFD designs with the same ME4 under the same flow and flux conditions, and the same conclusion applies to general class of ME*n* modules.

Since the principal targets of the BWRO industry are aimed at high recovery low-energy processes to save water and energy, and minimize handling needs of brine effluents, the attainment of such goals economically with simple CCD designs comprising ME4 is highly favours over the existing double-stage conventional SWRO systems with ME6 and turbocharge means, which are confined to ~80% recovery and operate with greater power needs and higher propensity to fouling and scaling. In CCD, recycled concentrates are continuously diluted with fresh feed at modules inlet with cross flow controlled independent of flux and system recovery; thereby, allow reaching critical values of foulants and scalants at very high recovery, and in some cases even operate briefly under supersaturation conditions of a certain constituent such as for example silica [24,25].

In contrast to conventional PFD techniques, CCD operate under fixed-flow and consecutive sequential pressure variations conditions that might raise a concern regarding the performance durability of membranes. Nevertheless, fixed-flow and variable pressure conditions imply a constant net driving pressure of operation of unchanged flow and flux at the level of each membrane in the module by exact analogy to conventional PFD techniques. Permeates' TDS derived by high recovery low-energy CCD of BW are more than sufficient for most applications, although being inferior to those of expensive multi-stage PFD techniques. It should however be pointed out that production of high quality permeates for specific applications makes use of domestic supply lines, or alike, as feed and proceeds by either conventional PFD or CCD techniques.

Acknowledgements

Funds to Desalitech Ltd. by AQUAGRO FUND L.P. (Israel) and by Liberation Capital LLC (USA) and Spring Creek Investments (USA) are gratefully acknowledged.

References

[1] K.H. Mistry, R.K. McGovern, G.P. Thiel, E.K. Summers, S.M. Zubair, J.H. Lienhard, Entropy generation analysis of desalination technologies, Entropy, 13 (2011) 1829–1864.
[2] N. Voutchkov, Membrane Seawater Desalination – Overview and Recent Trends, IDA Conference, Riverside, CA, USA, 2010.
[3] S. Loeb, S. Sourirajan, Advances in Chemistry Series, American Chemical Society, Vol. 38, 1963, pp. 117–132.

[4] M. Elimelech, W.A. Phillip, The future of seawater desalination: energy, technology, and the environment, Science, 333 (2011) 712–717.
[5] A. Efraty, R.N. Barak, Z. Gal, Closed circuit desalination – a new low energy high recovery technology without energy recovery, Desal. Wat. Treat., 31 (2011) 95–101.
[6] A. Efraty, R.N. Barak, Z. Gal, Closed circuit desalination series no-2: new affordable technology for sea water desalination of low energy and high flux using short modules without need of energy recovery, Desal. Wat. Treat., 42 (2012) 189–196.
[7] A. Efraty, Closed circuit desalination series no-6: conventional RO compared with the conceptually different new closed circuit desalination technology, Desal. Wat. Treat., 41 (2012) 279–295.
[8] A. Efraty, Closed circuit desalination series no-8: record saving of RO energy by SWRO-CCD without need of energy recovery, Desal. Wat. Treat., 52 (2014) 5717–5730.
[9] A. Efraty, CCD series no-11: single module compact SWRO-CCD units of low energy and high recovery for seawater desalination including with solar panels and wind turbines, Desal. Wat. Treat., 53 (2015) 1162–1176.
[10] A. Efraty, CCD series no-13: illustrating low energy SWRO-CCD of 60% recovery and BWRO-CCD of 92% recovery with a single element module without ER means – a theoretical extreme case study, Desal. Wat. Treat., 57 (2016) 9148–9165.
[11] A. Efraty, CCD series no-14: illustration of SWRO-CCD with fixed-pressure and variable flow instead of fixed-flow and variable pressure conditions, Desal. Wat. Treat., 56 (2015) 875–893.
[12] A. Efraty, CCD series no-15: simple design batch SWRO-CCD units for high recovery and low energy without ERD over a wide flux range of high cost effectiveness, Desal. Wat. Treat., 57 (2016) 9166–9179.
[13] A. Efraty, CCD series no-16: opened versus closed circuit SWRO batch desalination for volume reduction of silica containing effluents under super-saturation conditions, Desal. Wat. Treat., 57 (2016) 9569–9584.
[14] Z. Gal, A. Efraty, CCD series no-18: record low energy in closed circuit desalination of Ocean seawater with nanoH_2O elements without ERD, Desal. Wat. Treat., 57 (2016) 9180–9189.
[15] A. Efraty, CCD series no-19: the lowest energy prospects for SWRO through single-element modules under plug-flow and closed-circuit desalination conditions, Desal. Wat. Treat., 57 (2016) 21696–21711.
[16] A. Efraty, Closed circuit desalination series no-3: high recovery low energy desalination of brackish water by a new two-mode consecutive sequential method, Desal. Wat. Treat., 42 (2012) 256–261.
[17] A. Efraty, Closed circuit desalination series no-4: high recovery low energy desalination of brackish water by a new single stage method without any loss of brine energy, Desal. Wat. Treat., 42 (2012) 262–268.
[18] A. Efraty, J. Septon, Closed circuit desalination series no-5: high recovery, reduced fouling and low energy nitrate decontamination by a cost effective BWRO-CCD method, Desal. Wat. Treat., 49 (2012) 384–389.
[19] A. Efraty, Z. Gal, Closed circuit desalination series no 7: retrofit design for improved performance of conventional BWRO systems, Desal. Wat. Treat., 41 (2012) 301–307.
[20] A. Efraty, Closed circuit desalination series no-9: theoretical model assessment of the flexible BWRO-CCD technology for high recovery, low energy and reduced fouling applications, Desal. Wat. Treat., 53 (2015) 755–1779.
[21] A. Efraty, CCD series no-10: small compact BWRO-CCD units of high recovery, low energy and reduced fouling for supplied water upgrade to industry, irrigation, domestic and medical applications, Desal. Wat. Treat., 53 (2015) 1145–1161.
[22] A. Efraty, Closed circuit desalination series no-12: the use of 4, 5 and 6 element modules with the BWRO-CCD technology for high recovery, low energy and reduced fouling applications, Desal. Wat. Treat., 53 (2015) 1780–1804.
[23] J. Septon, A. Efraty, CCD series no-17: application of the BWRO-CCD technology for high recovery low energy desalination of domestic effluents, Desal. Wat. Treat., 57 (2016) 9585–9601.
[24] Z. Gal, J. Septon, A. Efraty, A.-M. Lee, CCD series no-20: high flux low energy upgrade of municipal water supplies with 96% recovery for boiler-feed and related applications, Desal. Wat. Treat., 57 (2016) 20219–20227.
[25] V. Sonera, J. Septon, A. Efraty, CCD series no-21: illustration of high recovery (93.8%) of a silica containing (57 ppm) source by a powerful technology of volume reduction prospects, Desal. Wat. Treat., 57 (2016) 20228–20236.
[26] Dow Liquid Separation, FILMTECTM Reverse Osmosis Membranes, Technical Manual, System Design, 2011, pp. 72–102. Available at: http://msdssearch.dow.com
[27] S. Lin, M. Elimelech, Staged reverse osmosis operation: configuration, energy efficiency, and application potential, Desalination, 366 (2015) 4–9.